BepiColombo observations of cold oxygen and carbon ions in the flank of the induced magnetosphere of Venus

L Z Hadid, Dominique Delcourt, Y Saito, M Fränz, S Yokota, B Fiethe, C Verdeil, B Katra, François Leblanc, H Fischer, et al.

nature astronomy

Article

https://doi.org/10.1038/s41550-024-02247-2

BepiColombo observations of cold oxygen and carbon ions in the flank of the induced magnetosphere of Venus

Received: 28 April 2022

Accepted: 11 March 2024

Published online: 12 April 2024

Check for updates

L. Z. Hadid[1] ✉, D. Delcourt[1,2], Y. Saito[3], M. Fränz[4], S. Yokota[5], B. Fiethe[6], C. Verdeil[7], B. Katra[1], F. Leblanc[1], H. Fischer[4], M. Persson[7,8], S. Aizawa[1], N. André[7], Y. Harada[9], A. Fedorov[7], D. Fontaine[1], N. Krupp[4], H. Michalik[6], J-J. Berthelier[10], H. Krüger[4], G. Murakami[3], S. Matsuda[11], D. Heyner[12], H.-U. Auster[12], I. Richter[12], J. Z. D. Mieth[12], D. Schmid[13] & D. Fischer[13]

On 10 August 2021, the Mercury-bound BepiColombo spacecraft performed its second fly-by of Venus and provided a short-lived observation of its induced magnetosphere. Here we report results recorded by the Mass Spectrum Analyzer on board Mio, which reveal the presence of cold O^+ and C^+ with an average total flux of ~$4 \pm 1 \times 10^4$ cm^{-2} s^{-1} at a distance of about six planetary radii in a region that has never been explored before. The ratio of escaping C^+ to O^+ is at most 0.31 ± 0.2, implying that, in addition to atomic O^+ ions, CO group ions or water group ions may be a source of the observed O^+. Simultaneous magnetometer observations suggest that these planetary ions were in the magnetosheath flank in the vicinity of the magnetic pileup boundary downstream. These results have important implications regarding the evolution of Venus's atmosphere and, in particular, the evolution of water on the surface of the planet.

During its formation, Venus was similar to Earth in many ways, including the existence of substantial amounts of liquid water[1,2]. However, Venus eventually evolved in a divergent way, leading to substantial differences between the two planets. Unlike Earth, Venus is now an extremely dry planet that lacks an intrinsic magnetic field. The continuous impact of the solar wind on the atmospheres of both planets results in important atmospheric losses[3–5]. The atmosphere of Venus, predominantly composed of carbon dioxide with smaller amounts of nitrogen and other minor species, is affected by interactions with the solar wind, leading to important ion outflows[6–9]. Therefore, studying and characterizing the present escape of ions from Venus is important for understanding the evolution of its atmosphere, and in particular, the evolution of water on the surface of the planet. Such studies may also provide insights into the general climate and habitability evolution of terrestrial planets and exoplanetary systems[10].

Our current understanding of the plasma environment around Venus is rooted in several pioneering missions. Mariner 2 (1962–1963)[11] was the first successful mission to establish the absence of an internal magnetic field in Venus. Venera 4 (1967) provided further information by conducting the first measurements of the planet's ionosphere during its descent into the atmosphere. Subsequently, Pioneer Venus Orbiter (PVO, 1978–1992) systematically mapped the various regions of

[1]LPP, CNRS, Observatoire de Paris, Sorbonne Université, Université Paris Saclay, École polytechnique, Institut Polytechnique de Paris, Palaiseau, France. [2]LPC2E-CNRS-CNES-Orléans University, Orléans, France. [3]ISAS-JAXA, Sagamihara, Japan. [4]Max Planck Institute for Solar System Research (MPS), Göttingen, Germany. [5]Osaka University, Osaka, Japan. [6]IDA, Braunschweig, Germany. [7]IRAP-CNRS-CNES-Toulouse University, Toulouse, France. [8]Graduate School of Frontier Sciences, The University of Tokyo, Kashiwa, Japan. [9]Kyoto University, Kyoto, Japan. [10]LATMOS-CNRS-IPSL, Paris, France. [11]Graduate School of Natural Science and Technology, Kanazawa University, Kanazawa, Japan. [12]Institut für Geophysik und extraterrestrische Physik, Technische Universität Braunschweig, Braunschweig, Germany. [13]Space Research Institute, Austrian Academy of Sciences, Graz, Austria. ✉e-mail: lina.hadid@lpp.polytechnique.fr

https://doi.org/10.1038/s41550-024-02247-2

interaction between the Sun and Venus and their boundaries[7]. These regions include the bow shock and magnetosheath generated by the interaction of the supersonic solar wind and the magnetic barrier region separating the shocked solar wind plasma and planetary ions[12]. The upstream boundary of the magnetic barrier is commonly referred to as the magnetic pileup boundary (MPB)[13–15]. Despite the restricted energy range of the Orbiter Plasma Analyzer[16] on board PVO, H^+ and O^+ were revealed to be the dominant ion species above 200 km altitude and were shown to escape tailward[17–20]. More complete ion composition measurements date from the Venus Express spacecraft (VEx, 2006–2014). Its highly polar orbits and comprehensive plasma package, Analyser of Space Plasmas and Energetic Atoms (ASPERA-4)[21], allowed detailed investigations of the low-altitude terminator and the mid-magnetotail regions up to a distance of about four planetary radii, which were not covered by the PVO mission (Fig. 1). One of its major findings was the absolute number of escaping hydrogen, helium and oxygen ions. In particular, it was shown that the ratio of escaping hydrogen to oxygen is about 2.6, which indicates that water is a major source of these ions[22,23]. Moreover, the flux of the escaping heavy ions with mass-to-charge ratio $m/q \geq 16$, which includes O^+, O_2^+ and CO_2^+, were observed during the solar minimum to be about three orders of magnitude larger in the mid-magnetotail region (~10^8 cm^{-2} s^{-1}) than in the magnetosheath flank (~10^5 cm^{-2} s^{-1}) with a total average escape rate of about $5.2 \pm 1.0 \times 10^{24}$ s^{-1} (ref. 24). Even though extensive statistical studies and reliable ion measurements were conducted, it was not possible to differentiate heavy species such as C^+, N^+, O_2^+ and CO_2^+ from O^+ because of the limited mass resolution of the ion mass analyser of the ASPERA-4 instrument suite. So far, no evidence of C^+ in the near Venus environment has been reported, except during a rare crossing of the planet's ionotail by the Solar and Heliospheric Observatory (SOHO) spacecraft in 1996 at the first Lagrangian point in the Earth–Sun system, which was as far as 45 million km from the planet[25]. The flux of escaping 15 keV (15 eV with respect to the mean proton energy) O^+ and C^+ ions was reported to be of the order of 2×10^3 cm^{-2} s^{-1}, with an abundance of C^+ to O^+ of ~10%.

Most of the heavy ions in Venus's ionosphere are cold (and slow moving). However, some of them are accelerated up to the escape velocity (10 km s^{-1}) or above (refs. 26,27 and references therein). The forces at work here involve: (1) the electric fields acting on ions, including the convective field of the solar wind (pickup process), (2) fields resulting from pressure gradients ('polar' wind), (3) an induced electric field ($\mathbf{J} \times \mathbf{B}$ force) and (4) fields of electromagnetic waves (wave–plasma interactions).

Results

Here we report the first in situ observations made by BepiColombo's Mass Spectrum Analyzer (MSA) and Mercury Ion Analyzer (MIA) during the spacecraft's second Venus fly-by on 10 August 2021. The two sensors are part of the Mercury Plasma Particle Experiment (MPPE)[28,29]. Although MIA is a toroidal top-hat electrostatic energy analyser that measures ions without mass distinction, MSA combines a spherical top-hat electrostatic energy analyser with a polarized time-of-flight (TOF) chamber ('reflectron' type) to allow for ion measurements with enhanced mass resolution. The combined observations of MSA and MIA provide insights into the flow of cold planetary ions and the underlying escape process in the distant flank of Venus's magnetosphere.

During this second fly-by, BepiColombo travelled into Venus's induced magnetosphere from dawn to dusk in the nightside northern hemisphere, with an inbound bow-shock crossing around 12:00 UT. It had its closest approach at 13:52 UT at an altitude of 552 km. It then crossed the bow-shock outbound at 14:01 UT and continued upstream in the solar wind (Fig. 1). Importantly, due to the 'stacked configuration' of BepiColombo during the cruise, the Magnetospheric Orbiter Sunshield and Interface Structure significantly obstructed the field of view (FOV) of all the particle sensors. In fact, only two entrance windows of MSA, which point along the +Z axis of BepiColombo, recorded the ion flux (see Fig. 4 in ref. 28). The MSA observation sequence started at 12:28 UT and lasted until 13:49 UT, at which point a 'safe mode' automatic procedure turned the instrument off due to the detection of an exceedingly large ion flux by MIA (ref. 29), as shown in Fig. 2e. During

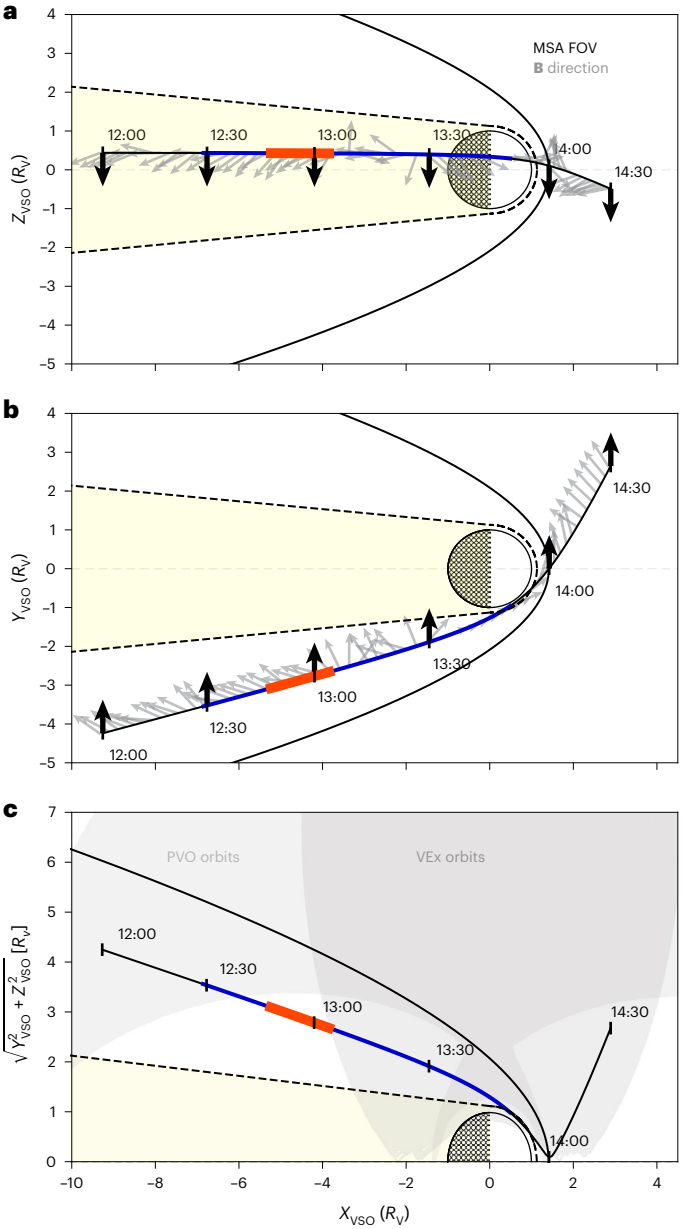

Fig. 1 | Trajectory of BepiColombo through the Venusian system on 10 August 2021 in VSO coordinates. The trajectory is shown in (**a**) $X_{VSO}Z_{VSO}$ (**b**) $X_{VSO}Y_{VSO}$ and (**c**) $X_{VSO}\sqrt{Y_{VSO}^2 + Z_{VSO}^2}$ planes. The VSO system is analogous to geocentric solar ecliptic coordinates. X_{VSO} is directed from the centre of the planet towards the Sun, Z_{VSO} is normal to the Venus orbital plane and positive towards the north celestial pole, and Y_{VSO} is positive in the direction opposite to the orbital motion. All dimensions are expressed in terms of Venus radii (R_V = 6,051 km). An empirically derived estimate of the bow-shock location[48] is shown as black solid lines. An estimate of the induced magnetospheric boundary (sometimes referred to as the upper mantle boundary)[49] is shown as black dashed lines for reference. The portion of the orbit highlighted in blue corresponds to the trajectory of BepiColombo during which MSA was operating (12:28–13:49 UT). The segment in red (12:47–13:04 UT) corresponds to the time interval during which low-energy planetary ions were observed. The black and grey arrows indicate the viewing direction of MSA and the magnetic field direction during the fly-by, respectively. The light grey and dark grey curves represent PVO (1984–1988) and VEx (2006-2010) trajectories during the solar minimum, respectively.

https://doi.org/10.1038/s41550-024-02247-2

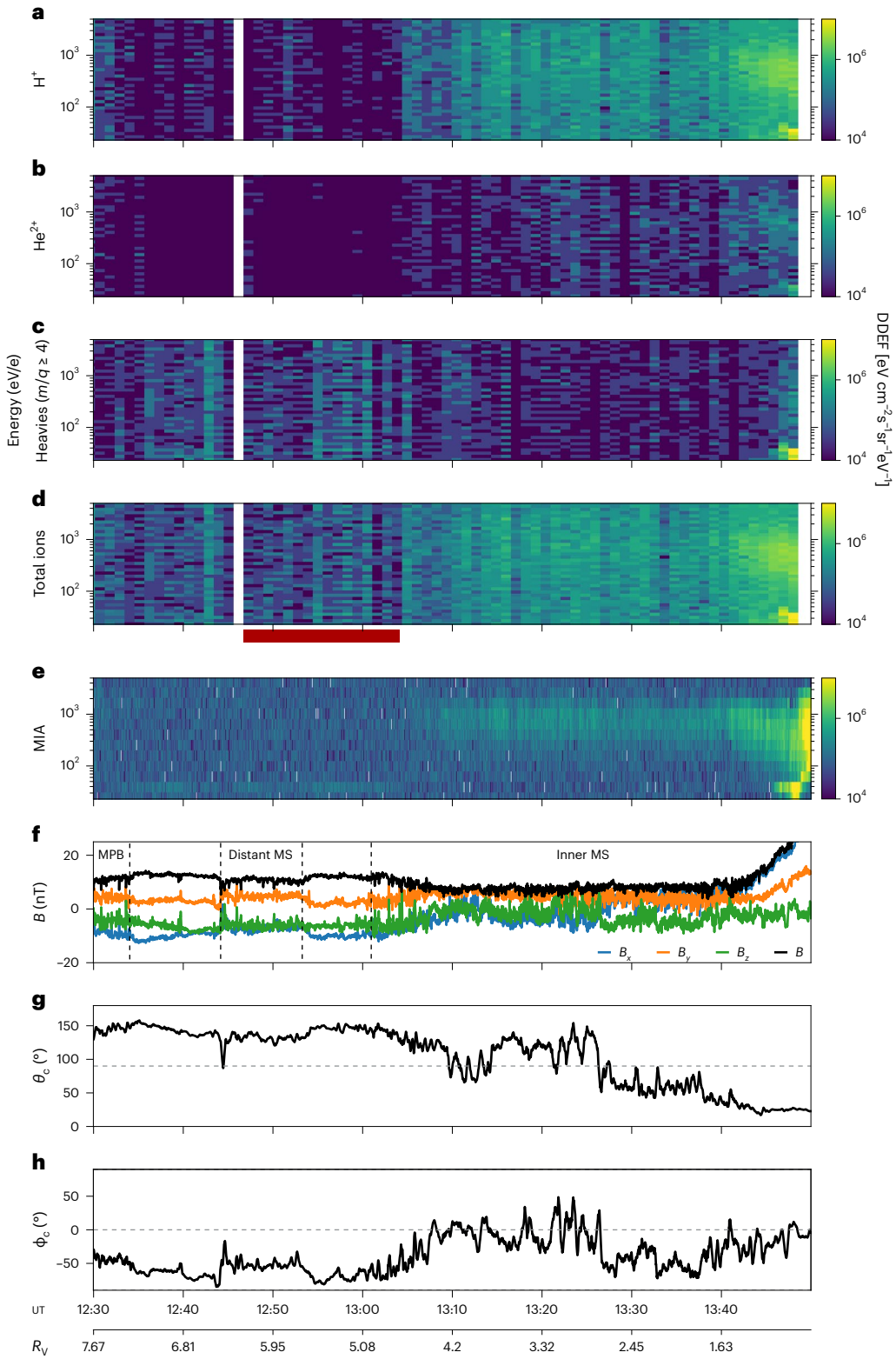

Fig. 2 | Ion energy–time spectrograms and magnetic field data in Venus's magnetosheath during the inbound part of BepiColombo's second fly-by. **a**–**h**, MSA protons (**a**), MSA alphas (**b**), MSA heavies (**c**), MSA total ions (**d**), MIA ions (**e**), magnetic field components and magnitude in the VSO coordinate system (**f**), cone angle θ_c (**g**) and clock angle ϕ_c (**h**). The red segment between **d** and **e** shows the MSA TOF observation sequence between 12:47 UT and 13:04 UT during which the composition of the heavy ions was identified (Fig. 3). Note the good agreement between the total MSA and MIA DDEF spectra after 13:40 UT (**d** and **e**). The vertical dashed lines in **f** represent the MPBs encountered by BepiColombo in the vicinity of the distant magnetosheath (MS).

this 91 min observation interval (red line in Fig. 1), the count rate matrices (H^+, He^{2+} as well as heavy ions, $m/q \geq 4$) were acquired at a cadence of 66 s, whereas the TOF spectra of straight-through particles in low mode (referred hereafter as TSTL) were accumulated during 1,024 s (ref. 28). Note that because of the limited telemetry rate, some data packets were lost during this observation sequence and only three

TSTL products were effectively acquired inside the magnetosphere of Venus between 12:28 UT and 13:49 UT.

MSA and MIA ion observations and magnetic field data

The observation sequence for MSA before the closest approach is displayed in Fig. 2. An increase of the H^+ differential directional energy flux (DDEF) can be seen at ~13:08 UT and ~13:40 UT (Fig. 2a) and signatures of He^{2+} ions around 400 eV can be noticed between 13:45 UT and 13:49 UT (Fig. 2b) as BepiColombo was approaching the planet. These H^+ and He^{2+} ion populations, which probably originated from the solar wind, are confirmed by the MIA instrument, which also revealed a maximum DDEF intensity near closest approach (Fig. 2e). Moreover, an increase of the heavy-ion flux is observed in the 12:30–13:08 UT time interval (also confirmed by MIA near 20 eV) and closer to the planet around 13:49 UT (Fig. 2c). Note that the vertical spread of the DDEF with respect to energy in Fig. 2a–d is an artefact from the software version used by MSA at the time of the fly-by. To support these ion measurements, magnetic field data from the magnetometer on board the Mercury Planetary Orbiter (MPO-MAG)[30,31] is included in Fig. 2f. It is apparent from this latter panel that the sharp increase of the proton DDEF in the magnetosheath flank at ~13:08 UT (Fig. 2a) coincided with a change in the magnetic field orientation and magnitude. More specifically, after ~13:08 UT, the magnetic field magnitude decreased, the cone (θ_c, Fig. 2g) and the clock angle (ϕ_c, Fig. 2h) changed from ~147° (anti-sunward) and approximately −70° (southward) to ~96° (perpendicular to the Venus–Sun line) and approximately −2° (eastward), respectively. Keeping in mind that the nominal Parker spiral angle at Venus is ~144°/36°, this implies that until ~13:08 UT, the magnetic field was nearly along the Parker direction. The sharp changes of the magnetic field orientation and the ion DDEF suggest that there was a crossing of different regions in the plasma environment of Venus. The consecutive increase in the field components around 12:40 UT and 13:00 UT (consistent with an increase in draping[32]) and the suppression of the magnetosheath wave activity strongly indicate that BepiColombo moved across the MPB, where it subsequently observed the cold ion outflow. From 13:08 UT until 13:40 UT, along with the appearance of kilo-electronvolt ions, the spacecraft was in the dayside magnetosheath flank and got closer to the induced magnetospheric boundary after 13:40 UT (Fig. 1).

MSA TOF analysis

Due to the low signal-to-noise ratio of MSA data during this encounter and the low mass resolution of the count rate matrices during the cruise, heavy ions cannot be clearly identified from the corresponding energy–time spectrograms (Fig. 2). However, identifying these ions is possible from the acquired TOF spectra. During this fly-by, only two TOF spectra were acquired inside Venus's induced magnetosheath, in the time intervals 12:47–13:04 UT and 13:04–13:22 UT. The first TOF spectrum (in the distant magnetosheath) is shown in Fig. 3. The ion TOFs were measured for 2,000 TOF channels of 0.78125 ns each. The histogram in Fig. 3 shows the data between 12:47 and 13:04 UT as groups of 24 TOF channels and are compared with MSA calibration profiles for O^+ and C^+ (green and orange curves, respectively). Note that the MSA raw data were obtained by integrating counts up to 1 keV, although most of these ions have an energy of only ~18 eV (described in more details in Methods), consistent with MIA observations (Fig. 2e). The histogram shown in this figure exhibits several peaks of particular interest. Indeed, although the peaks near 423 and 557 ns reflect the presence of O^+ (with a 95% confidence level, confidence intervals are [417, 462] ns and [532, 587] ns, respectively), the additional peak in the 460–530 ns interval denotes the presence of C^+ (confidence interval of [486, 513] ns). Note the slight deviation between the calibrated carbon peak and the observed one. At the time of writing, the reason for this deviation is unclear (possibly due to instrumentation, calibration methodology or counts statistics). These well-defined peaks provide clear evidence of planetary heavy ions in the distant magnetosheath flank, a region

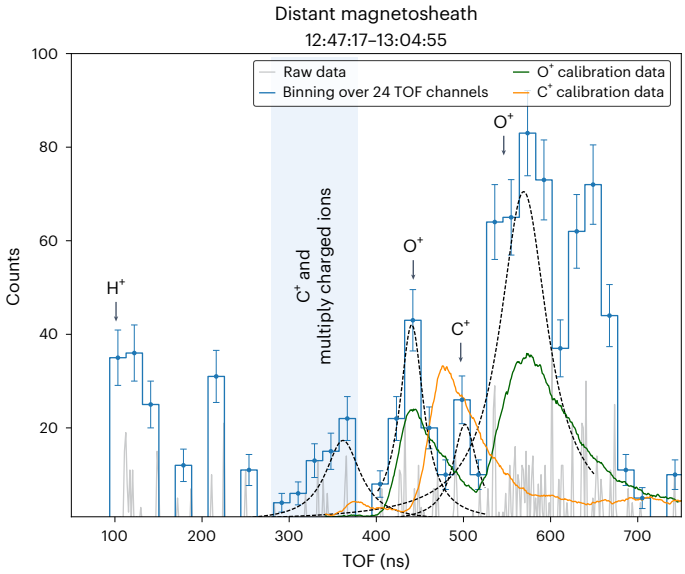

Fig. 3 | Total counts versus ion TOFs. Counts were recorded for Venus's induced magnetosheath during the second gravity-assist manoeuvre of BepiColombo on 10 August 2021 in the time interval 12:47–13:04 UT. The grey profiles show the data obtained using the full TOF resolution of MSA (namely, 2,000 TOF channels of 0.78125 ns each). The blue histogram represents a binning of these data summed within bins of 24 TOF channels. The error bars along the blue profiles depict the 1σ deviation of the measurements assuming a Poisson-like distribution. Each point and relative error bar refer to the sum and plus or minus the standard deviation. The green and orange curves represent the MSA calibration of O^+ and C^+, respectively, for a voltage of ±8 kV applied inside the TOF chamber. The peaks highlighted in the grey area at TOF >600 ns represents ions with $m/q \geq 28$ AMU e^{-1}, which may be due to Si^+ or other complex ions emitted from the spacecraft.

that has never been explored before. For comparison, the leftmost and rightmost panels in Fig. 4 show histograms before and after the time interval shown in Fig. 3. It is clear from the left-hand (Fig. 4a) and right-hand (Fig. 4c) panels that there is no clear evidence of heavy-ion species in contrast to the centre panel (Fig. 4b). Note that no changes in the spacecraft attitude were observed during this observation period. This confirms that most of the ions observed between 12:47 UT and 13:04 UT were not due to the spacecraft outgassing or sputtering. Furthermore, in the centre panel of Fig. 4, the second peak associated with O^+ appears broadened by another peak between 610 and 700 ns. This additional peak corresponds to a mass-to-charge ratio of approximately 28 atomic mass units (AMU) per electron charge (for singly charged ion species), which could be due to the presence of molecular ions like CO^+ and N_2^+. However, the densities of these molecular ions are noticeably lower than that of O^+ above 200 km, and their molecular form was unlikely to be observed by MSA at ~6R_V due to dissociative recombination[33]. Note that these signatures could be caused as well by Si^+ or other complex ions emitted from the spacecraft, for example, due to Mio's optical specular reflector outgassing or sputtering[34]. The peak in the 300–380 ns interval is probably due to a combination of two contributions: (1) a minor contribution of negative carbon ions (see caption of Fig. 3) and (2) a substantial contribution of multiply charged heavy ions that experience a post-acceleration higher than that of C^+ before entering the MSA TOF chamber; hence, they have shorter TOFs than those of C^+. Precise identification of these multiply charged ions species will require further investigation based on both experimental datasets and numerical modelling, which is out of the scope of the present study. By fitting the peaks of the TOF spectra with Lorentzian distributions (dashed lines in Fig. 3; see Methods for more details), we can integrate the total counts and get an estimate of the density fraction of C^+ with respect to O^+. Overall, the abundance of carbon relative

https://doi.org/10.1038/s41550-024-02247-2

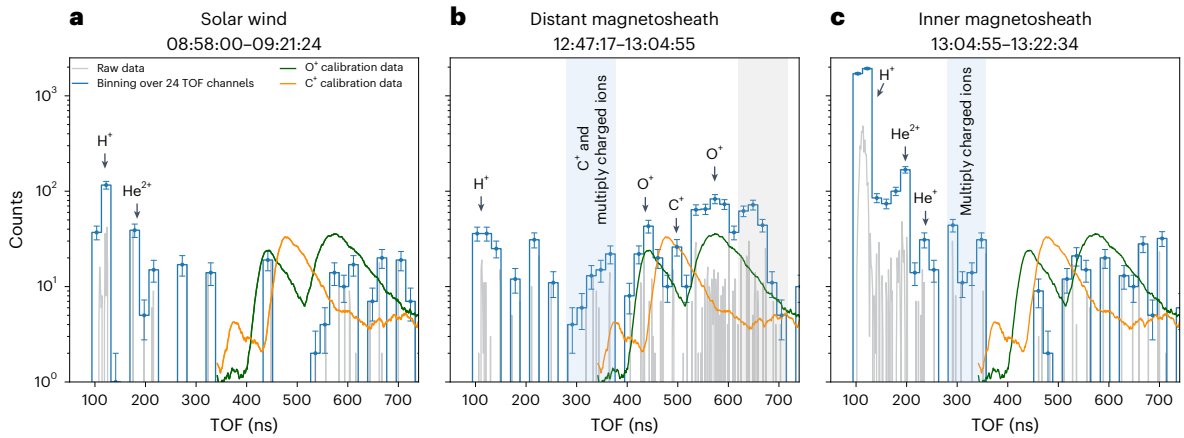

Fig. 4 | Three consecutive TOF spectra recorded during the second gravity-assist manoeuvre of BepiColombo on 10 August 2021. a, In the solar wind upon approach to Venus's induced magnetosphere. **b**,**c**, In Venus's induced magnetosheath in the time intervals 12:47–13:04 UT (**b**) and 13:04 UT–13:22 UT (**c**). The grey profiles show the data obtained using the full TOF resolution of MSA (namely, 2,000 TOF channels each of 0.78125 ns). The blue histograms represent a binning of these data summed within bins of 24 TOF channels. The error bars along the blue profiles depict the 1σ deviation of the measurements assuming a Poisson-like distribution. Each point and relative error bar refer to the sum and plus or minus the standard deviation. The format is identical to that of Fig. 3.

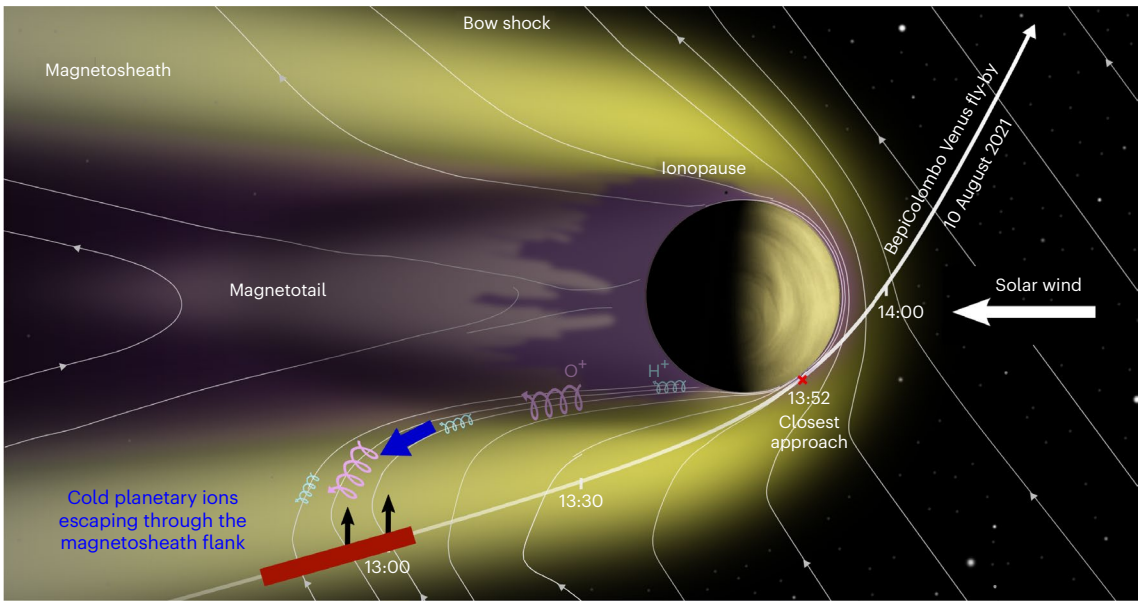

Fig. 5 | Schematic view of planetary material escaping through Venus's magnetosheath flank. The illustration is of the X–Y_{VSO} plane with a cut at $Z_{VSO} = 0$. The red segment shows the MSA observation sequence between 12:47 UT and 13:04 UT. The black arrows represent the FOV of MSA, and the blue arrow reflects the ions escaping at an angle of ~140° with the magnetic field lines (the angle is calculated using the FOV of MSA). Unlike other observation sequences, during this time window the incoming ions were moving in the same direction as the MSA FOV. The open magnetic field lines were obtained using the global hybrid model LatHyS (Latmos Hybrid Simulation[50]), with input parameters (for example, density, velocity, proton temperature and clock angle) constrained by Solar Orbiter observations in the upstream solar wind[51]. The polar view of Venus was taken from the Venus Monitoring Camera (VMC) onboard Venus Express (credits: ESA/MPS).

to oxygen is at most 31% ± 21%, which is higher than the previously reported abundance of C^+ to O^+ of about 10% (ref. 25). This suggests that the observed oxygen ions are due to a combination of (1) atomic O^+ released from the ionosphere, (2) the dissociation of CO or water group ions and (3) the dissociation of molecular O_2^+ ions that broke up when crossing the MSA carbon foil. Note that closer to the planet, the composition of the intense ion flux observed by MSA near 20 eV (Fig. 2d) cannot be investigated due to the lack of TSTL data.

Discussion

Although previous measurements of cold planetary oxygen were mostly obtained in the ionotail close to Venus, the MSA data presented here provide evidence of cold heavy ions of planetary origin (O^+ and C^+) in the flank of Venus's induced magnetosphere, in the vicinity of the upstream MPB. To obtain the total flux, the DDEF was integrated between 12:40 UT and 13:04 UT over the various energy steps of MSA and solid angle. To do so, the measured flux was considered to be obtained from only two MSA entrance windows looking along the spacecraft's Z axis (see above) and an isotropic ion distribution was assumed. This yielded an average flux of ~$4 \pm 1 \times 10^4$ cm^{-2} s^{-1}. As noted earlier, previous studies could not distinguish the heavy ions. Nevertheless, a higher flux was reported in the magnetosheath flank closer to Venus ~$3R_V$ (~1×10^5 cm^{-2} s^{-1})[24], and a lower one was reported in the ionotail further away from the planet ~$7{,}500R_V$ (~$2.4–4.4 \times 10^3$ cm^{-2} s^{-1})[25].

The lack of high-resolution field and particle measurements during this fly-by hinders a thorough analysis of the escape process for the planetary ions. However, the estimate of the pitch angle of approximately 140° made using the MSA FOV (Fig. 5) suggests that the

ions predominantly flow outwards and parallel to the magnetic field, rather than perpendicular to it. Therefore, it is unlikely that these ions are pickup ions. Furthermore, considering the low energy of these observed ions (~18 eV), a plausible explanation for their escape is a process similar to the 'polar-wind', in which the thermal pressure gradient and the gravitational separation of ions and electrons along the magnetic field lines set up an ambipolar electrostatic field that accelerates ions towards electrons. As a result, there is an upward flow of ionospheric material[35–37]. Note that measurements made by VEx indicate the formation of an electric field in the Venusian upper ionosphere with a strength of approximately 9.9 V. This electric field can accelerate any ion lighter than 18 AMU to escape velocities[38,39]. Note that C^+ and O^+ ions would have escape energies of 6.3 and 8.4 eV, respectively, if they were released in the vicinity of the planet's surface. Furthermore, it has been estimated that the spacecraft potential was approximately 9 V during this fly-by[40]. Consequently, these ions would have undergone an energization of no more than 30 eV before reaching MSA. This indicates that the spacecraft potential plays an insignificant role in accelerating the ions compared to the ambipolar electrostatic field. An alternative explanation to ion acceleration by the ambipolar electric field could be the centrifugal energization (a few tens of electronvolts) experienced by ions as they flow away from the planet due to the $\mathbf{E} \times \mathbf{B}$ convection of the magnetic field lines, as described, for example, in ref. 41.

In conclusion, the science opportunity offered by the second Venus fly-by of BepiColombo allowed us to investigate to some extent the ion composition of Venus's magnetospheric flank. The present study demonstrates the presence of cold (~18 eV) heavy planetary ions (C^+ and O^+) with an average total flux of ~$4 \pm 1 \times 10^4$ cm^{-2} s^{-1}. Although O^+ ions have been observed to outflow from Venus by previous spacecraft, this study provides the first evidence of escaping C^+ ions around six planetary radii. Modelling efforts are underway to further investigate the presence of cold heavy ions in the distant magnetosheath flank close to the MPB. Characterizing the loss of heavy ions and understanding the escape mechanisms for Venus are crucial for improving our knowledge regarding the water evolution on the surface of the planet, for determining the history of volatiles in our Solar System and for better constraining models of terrestrial exoplanets.

Methods

MSA instruments

The MSA is a high-mass-resolution ion spectrometer on board Mio, BepiColombo's magnetospheric orbiter. Being part of the MPPE, which is dedicated to particle measurements[29], MSA is designed to provide three-dimensional mass-resolved ion-phase space densities in Mercury's magnetosphere. This ion spectrometer combines a spherical top-hat analyser for energy analysis with a TOF chamber for mass analysis. At the entrance of the TOF analyser, the ions interact with carbon foils and, as a result of charge exchange, may exit as neutrals or positive or negative ions. Unlike most spectrometers on board spacecraft, such as the Fast Imaging Plasma Spectrometer on board MESSENGER[42,43], which has an equipotential TOF chamber, a prominent characteristic of MSA (from which derives its complexity) is that the TOF chamber is linearly polarized, which allows us to correct the energy and angular scattering upon entry of the positive ions into the TOF chamber[28]. This original 'reflectron' concept[44] leads to isochronous TOFs, hence, with an enhanced mass resolution ($m/\Delta m > 40$). Such performance has seldom been achieved with onboard mass spectrometers and will be particularly useful at Mercury because of the large variety of ions of planetary origin that circulate in its magnetosphere after ejection by different processes (for example, solar wind sputtering, thermal desorption or meteorite impact). On the other hand, most of the incoming ions measured by MSA exit the carbon foils as neutrals or negative ions. These ions have 'straight-through' trajectories towards the bottom end of the MSA TOF chamber (see Fig. 2 in ref. 28). Throughout the cruise phase, because of the limited telemetry rate, MPO and Mio data are produced at low resolution and only straight-through data produced by MSA are transmitted. It should be stressed here that not all ions entering the MSA TOF chamber display two peaks in straight-through spectra. Although one of these two peaks (the most prominent one) is due to ions that are neutralized upon crossing the carbon foil, the second peak (at shorter TOFs) is due to ions that exit the carbon foil negatively charged in substantial numbers, such as carbon or oxygen but not helium or argon. Because of the linear electric field applied inside the TOF chamber, these latter ions are rapidly accelerated towards the straight-through detector and, thus, have shorter TOFs than those of neutrals[28]; hence, two distinct peaks are present (as for the O^+ and C^+ ions), in contrast with the single peak obtained by an ion spectrometer with an equipotential TOF chamber[45].

Large structure of Venus's induced magnetosphere

To better understand the ion observations, we calculated the clock and cone angles of the magnetic field to identify the large-scale structure of Venus's induced magnetosphere. The cone (θ_c) and clock (ϕ_c) angles are defined as:

$$\theta_c = \tan^{-1}\left(\frac{\sqrt{B_y^2 + B_z^2}}{B_x}\right), \quad (1)$$

$$\phi_c = \tan^{-1}\left(\frac{B_z}{B_y}\right). \quad (2)$$

The Venus Solar Orbital (VSO) coordinate system is used, where X_{VSO} is along the Venus–Sun line, Y_{VSO} is in the opposite direction of Venus's orbital velocity and Z_{VSO} completes the triad and is along Venus's rotational axis. A cone angle of $\theta_c = 0°$ (180°) implies a sunward (anti-sunward) directed B field and $\theta_c = 90°$ is a field directed perpendicular to the Venus–Sun line. The clock angle ϕ_c is the direction of the magnetic field in the Y–Z VSO-plane with $\phi_c = 0°$ indicating an eastward pointing field and $\phi_c = 90°$ a northward one.

Histograms of the TOF spectra

Upon the entry of an ion into the MSA TOF chamber, a START pulse is produced by secondary electrons, which opens a TOF window of 1,562 ns and during which a STOP pulse is expected. Once the START and STOP pulses are acquired, the ion TOF in the chamber is computed with a time-to-digital converter resolution of 0.78125 ns (ref. 28). MSA TOF spectra were subsequently analysed by summing these different TOF channels. Supplementary Fig. 1 shows MSA TOF spectra between 250 and 750 ns and binned over 12 (light blue), 24 (medium blue) and 40 (dark blue) TOF channels. It is apparent from this figure that the C^- and C peaks persist using either 12 or 24 TOF channel binning, although not surprisingly, these features are noticeably attenuated if a bin size that is too wide (40 TOF channels) is used.

Estimating the heavy-ion energy

The bulk of the heavy-ion energy was estimated from MSA TOF spectra (from 12:47:17 UT to 13:04:55 UT) by integrating the counts within each TOF boundary up to 1 keV for $12 \le m/q \le 23$ (Supplementary Fig. 2). Since TOF spectra below 1 keV hardly depend upon the ion energy on entry into the instrument (due to post-acceleration up to 8 kV at the exit of the energy analyser), we have limited the analysis to 1 keV to exclude the effect of the energy spreading (Fig. 1).

Fitting the TOF spectrum

As mentioned in Main, because of limited counting statistics, we use a nonlinear least-squares method to fit the main peaks in the TOF spectra between 300 and 650 ns. The dispersion within the carbon foil is a random process that is expected to yield a velocity distribution

constrained by both a maximum and a minimum[28,46,47]. This primarily impacted the heavy-ion species by introducing a broadening in the TOF spectra at longer TOFs. When performing the nonlinear least-squares fit to the main peaks of the TOF spectra, we considered three different types of distributions, namely, Gaussian, log-normal and Lorentzian (also known as a Cauchy–Lorentz distribution). Although the three distributions fit the MSA data relatively well, we show in Fig. 3 the results obtained using the Lorentzian distribution, which better fitted the width of the TOF peaks. This function has the following shape:

$$f(x;A,\mu,\sigma) = \frac{A}{\pi}\left[\frac{\sigma}{(x-\mu)^2+\sigma^2}\right],$$

where the parameter amplitude corresponds to A, the centre to μ and the standard deviation to σ.

Calculation of uncertainties

The uncertainties in the binned TSTL spectra (Fig. 3) are due to counting (Poisson) statistics. Thus, the error ϵ is calculated assuming a Poisson distribution where $\epsilon = \sqrt{N}$ and N is the number of counts in each bin. The error on the abundance calculation of C^+/O^+ is calculated as:

$$\sqrt{\left(\frac{\sum \delta O^+}{\sum O^+}\right)^2 + \left(\frac{\sum \delta C^+}{\sum C^+}\right)^2}, \quad (3)$$

where δX and X represent, respectively, the standard deviation and the total counts of the corresponding Lorentzian fit for each species.

Data availability

The spacecraft orbit data are available from SPICE data for BepiColombo (https://www.cosmos.esa.int/web/spice/spice-for-bepicolombo)[52]. The MSA, MIA and MPO-MAG data are available from https://zenodo.org/records/10682832 (in a Zenodo repository)[53]. The MSA and MIA teams (Y. Saito, principal investigator; saito@stp.isas.jaxa.jp) and MPO-MAG team (D. Heyner, principal investigator; d.heyner@tu-bs.de) and the corresponding author can provide the MSA, MIA and MPO-MAG data upon reasonable request. All MPO observational data are available on Zenodo (https://zenodo.org/records/10925302)[54]. Source data are provided with this paper.

References

1. Bougher, S. W., Hunten, D. M. & Phillips, R. J. (eds) *Venus II: Geology, Geophysics, Atmosphere, and Solar Wind Environment* (Univ. of Arizona Press, 1997).
2. Lammer, H. et al. Origin and evolution of the atmospheres of early Venus, Earth and Mars. *Astron. Astrophys. Rev.* **26**, 2 (2018).
3. Strangeway, R. J., Ergun, R. E., Su, Y.-J., Carlson, C. W. & Elphic, R. C. Factors controlling ionospheric outflows as observed at intermediate altitudes. *J. Geophys. Res. Space Phys.* **110**, A3 (2005).
4. Nilsson, H., Barghouthi, I. A., Slapak, R., Eriksson, A. I. & André, M. Hot and cold ion outflow: spatial distribution of ion heating. *J. Geophys. Res. A, Space Phys.* **117**, A11 (2012).
5. Schillings, A. et al. Earth atmospheric loss through the plasma mantle and its dependence on solar wind parameters. *Earth Planets Space* **71**, 70 (2019).
6. Luhmann, J. G. The solar wind interaction with Venus. *Space Sci. Rev.* **44**, 241–306 (1986).
7. Russell, C. T., Luhmann, J. G. & Strangeway, R. J. The solar wind interaction with Venus through the eyes of the Pioneer Venus Orbiter. *Planet. Space Sci.* **54**, 1482–1509 (2006).
8. Kollmann, P. et al. Properties of planetward ion flows in Venus' magnetotail. *Icarus* **274**, 73–82 (2016).
9. Ramstad, R. & Barabash, S. Do intrinsic magnetic fields protect planetary atmospheres from stellar winds? *Space Sci. Rev.* **217**, 36 (2021).
10. Kane, S. R. et al. Venus as a laboratory for exoplanetary science. *J. Geophys. Res. E, Planets* **124**, 2015–2028 (2019).
11. Smith, E. J., Davis, L., Coleman, P. J. & Sonett, C. P. Mariner II: preliminary reports on measurements of Venus: magnetic field. *Science* **139**, 909–910 (1963).
12. Zhang, T. L., Luhmann, J. G. & Russell, C. T. The magnetic barrier at Venus. *J. Geophys. Res. A, Space Phys.* **96**, 11145–11153 (1991).
13. Bertucci, C., Mazelle, C., Slavin, J. A., Russell, C. T. & Acuña, M. H. Magnetic field draping enhancement at Venus: evidence for a magnetic pileup boundary. *Geophys. Res. Lett.* **30**, 17 (2003).
14. Bertucci, C., Mazelle, C., Acuña, M. H., Russell, C. T. & Slavin, J. A. Structure of the magnetic pileup boundary at Mars and Venus. *J. Geophys. Res. A, Space Phys.* **110**, A1 (2005).
15. Kallio, E. et al. The Venusian induced magnetosphere: a case study of plasma and magnetic field measurements on the Venus Express mission. *Planet. Space Sci.* **56**, 796–801 (2008).
16. Intriligator, D. S., Wolfe, J. H. & Mihalov, J. D. The Pioneer Venus Orbiter plasma analyzer experiment. *IEEE Trans. Geosci. Remote Sens.* **GE-18**, 39–43 (1980).
17. Nagy, A. F., Cravens, T. E., Yee, J.-H. & Stewart, A. I. F. Hot oxygen atoms in the upper atmosphere of Venus. *Geophys. Res. Lett.* **8**, 629–632 (1981).
18. Mihalov, J. D. & Barnes, A. The distant interplanetary wake of Venus: plasma observations from Pioneer Venus. *J. Geophys. Res. Space Phys.* **87**, 9045–9053 (1982).
19. Knudsen, W. C., Miller, K. L. & Spenner, K. Median density altitude profiles of the major ions in the central nightside Venus ionosphere. *J. Geophys. Res.* **91**, 11936–11950 (1986).
20. Luhmann, J. G., Ledvina, S. A., Lyon, J. G. & Russell, C. T. Venus O^+ pickup ions: collected PVO results and expectations for Venus Express. *Planet. Space Sci.* **54**, 1457–1471 (2006).
21. Barabash, S. et al. The analyser of space plasmas and energetic atoms (ASPERA-4) for the Venus Express mission. *Planet. Space Sci.* **55**, 1772–1792 (2007).
22. Barabash, S. et al. The loss of ions from Venus through the plasma wake. *Nature* **450**, 650–653 (2007).
23. Fedorov, A. et al. Measurements of the ion escape rates from Venus for solar minimum. *J. Geophys. Res. A, Space Phys.* **116**, A7 (2011).
24. Nordström, T., Stenberg, G., Nilsson, H., Barabash, S. & Zhang, T. L. Venus ion outflow estimates at solar minimum: influence of reference frames and disturbed solar wind conditions. *J. Geophys. Res. Space Phys.* **118**, 3592–3601 (2013).
25. Grünwaldt, H. et al. Venus tail ray observation near Earth. *Geophys. Res. Lett.* **24**, 1163–1166 (1997).
26. Futaana, Y., Stenberg Wieser, G., Barabash, S. & Luhmann, J. G. Solar wind interaction and impact on the Venus atmosphere. *Space Sci. Rev.* **212**, 1453–1495 (2006).
27. Persson, M. et al. Heavy ion flows in the upper ionosphere of the Venusian north pole. *J. Geophys. Res. A, Space Phys.* **124**, 4597–4607 (2019).
28. Delcourt, D. et al. The Mass Spectrum Analyzer (MSA) on board the Bepicolombo MMO. *J. Geophys. Res. A, Space Phys.* **121**, 6749–6761 (2016).
29. Saito, Y. et al. Pre-flight calibration and near-Earth commissioning results of the Mercury Plasma Particle Experiment (MPPE) onboard MMO (Mio). *Space Sci. Rev.* **217**, 70 (2021).
30. Glassmeier, K.-H. et al. The fluxgate magnetometer of the BepiColombo Mercury Planetary Orbiter. *Planet. Space Sci.* **58**, 287–299 (2010).

31. Heyner, D. et al. The BepiColombo Planetary Magnetometer MPO-MAG: what can we learn from the Hermean magnetic field? *Space Sci. Rev.* **217**, 52 (2021).
32. Zhang, T. L. et al. Initial Venus Express magnetic field observations of the magnetic barrier at solar minimum. *Planet. Space Sci.* **56**, 790–795 (2008).
33. Fox, J. L. & Sung, K. Y. Solar activity variations of the Venus thermosphere/ionosphere. *J. Geophys. Res. A, Space Phys.* **106**, 21305–21335 (2001).
34. Schläppi, B. et al. Influence of spacecraft outgassing on the exploration of tenuous atmospheres with in situ mass spectrometry. *J. Geophys. Res. A, Space Phys.* **115**, A12 (2010).
35. Tsang, S. M. E. et al. Ionospheric photoelectrons at Venus: case studies and first observation in the tail. *Planet. Space Sci.* **113–114**, 385–394 (2015).
36. Coates, A. J. et al. Distant ionospheric photoelectron energy peak observations at Venus. *Planet. Space Sci.* **113–114**, 378–384 (2015).
37. Inui, S. et al. Cold dense ion outflow observed in the Martian-induced magnetotail by Maven. *Geophys. Res. Lett.* **45**, 5283–5289 (2018).
38. Collinson, G. A. et al. The electric wind of Venus: a global and persistent 'polar wind'-like ambipolar electric field sufficient for the direct escape of heavy ionospheric ions. *Geophys. Res. Lett.* **43**, 5926–5934 (2016).
39. Brecht, S. H. & Ledvina, S. A. An explanation of the nightside ionospheric structure of Venus. *J. Geophys. Res. A, Space Phys.* **126**, 2020–027779 (2021).
40. Rojo, M. et al. Electron moments derived from the Mercury Electron Analyzer during the cruise phase of BepiColombo. *Astron. Astrophys.* **683**, A99 (2024).
41. Delcourt, D. C., Seki, K., Terada, N. & Moore, T. E. Centrifugally stimulated exospheric ion escape at Mercury. *Geophys. Res. Lett.* **39**, 22 (2012).
42. Solomon, S. C., McNutt, R. L., Gold, R. E. & Domingue, D. L. MESSENGER mission overview. *Space Sci. Rev.* **131**, 3–39 (2007).
43. Raines, J. M. et al. Distribution and compositional variations of plasma ions in Mercury's space environment: the first three Mercury years of MESSENGER observations. *J. Geophys. Res. A, Space Phys.* **118**, 1604–1619 (2013).
44. Managadze, G. G. Time-of-flight mass-spectrometer. World patent 22058786 (1991); http://inis.iaea.org/search/search.aspx?orig_q=RN:22058786
45. Zurbuchen, T. H. et al. MESSENGER observations of the composition of Mercury's ionized exosphere and plasma environment. *Science* **321**, 90–92 (2008).
46. Allegrini, F. et al. Energy loss of 1–50 keV H, He, C, N, O, Ne, and Ar ions transmitted through thin carbon foils. *Rev. Sci. Instrum.* **77**, 044501 (2006).
47. Allegrini, F., Ebert, R. W. & Funsten, H. O. Carbon foils for space plasma instrumentation. *J. Geophys. Res. A, Space Phys.* **121**, 3931–3950 (2016).
48. Martinecz, C. et al. Location of the bow shock and ion composition boundaries at Venus–initial determinations from Venus Express ASPERA-4. *Planet. Space Sci.* **56**, 780–784 (2008).
49. Martinecz, C. et al. Plasma environment of Venus: comparison of Venus Express ASPERA-4 measurements with 3-d hybrid simulations. *J. Geophys. Res. E, Planets* **114**, E9 (2009); https://doi.org/10.1029/2008JE003174
50. Modolo, R. et al. The LatHys database for planetary plasma environment investigations: overview and a case study of data/model comparisons. *Planet. Space Sci.* **150**, 13–21 (2018).
51. Aizawa, S. et al. LatHys global hybrid simulation of the BepiColombo second Venus flyby. *Planet. Space Sci.* **218**, 105499 (2022).
52. *BepiColombo SPICE Kernels Set* (ESA, 2024); https://www.cosmos.esa.int/web/spice/spice-for-bepicolombo
53. Hadid, L. et al. BepiColombo/Mio MSA, MIA and MPO MAG data during the second Venus flyby. *Zenodo* https://zenodo.org/records/10682832 (2024).
54. Hadid, L. et al. BepiColombo/Mio MSA, MIA and MPO MAG data during the second Venus flyby. *Zenodo* https://zenodo.org/records/10925302 (2024).

Acknowledgements

We thank F. Leblanc, R. Modolo and M. Rojo for useful discussions. We also express our sincere thanks to all members of the Mio and BepiColombo mission for their careful contributions to the projects' operations and for their efforts in making the mission successful. This paper is based on observations obtained with BepiColombo, a joint European Space Agency (ESA)-Japan Aerospace Exploration Agency (JAXA) science mission with instruments and contributions directly funded by the ESA member states and JAXA. The French participation in the BepiColombo mission is funded by the French National Centre for Space Studies. The Europlanet 2024 Research Infrastructure's SPIDER activity has received funding from the European Union's Horizon 2020 research and innovation programme (Grant Agreement No. 871149). M.P. was funded by the European Union's Horizon 2020 programme (Grant Agreement No. 871149 for Europlanet 2024 Research Infrastructure). Work at the Max Planck Institute for Solar System Research is supported by the German Aerospace Centre (Contracts 50 QW 0503, 50 QW 1303, 50 QW 1702 and 50 QW 2101) and by the Max Planck Society. D.H. was supported by the German Federal Ministry for Economic Affairs and Climate Action and the German Aerospace Centre (Contract 50QW2202).

Author contributions

L.Z.H. and D.D. developed the scientific content of the study, analysed the data and wrote the initial draft of the manuscript. All authors have read and provided feedback on the manuscript. Y.S. is the principal investigator of the MPPE consortium. D.D. is a co-principal investigator of MPPE. N.A. is a lead co-investigator of MPPE. G.M. is JAXA's project scientist for BepiColombo Mio. D.H. is the principal investigator of MPO-MAG. The remaining co-authors are co-investigators on MSA, MIA, Mercury Electron Analyzer or MPO-MAG.

Competing interests

The authors declare no competing interests.

Additional information

Supplementary information The online version contains supplementary material available at https://doi.org/10.1038/s41550-024-02247-2.

Correspondence and requests for materials should be addressed to L. Z. Hadid.

Peer review information *Nature Astronomy* thanks Jim Raines and the other, anonymous, reviewer(s) for their contribution to the peer review of this work.